Korean J. Chem. Eng., 38(5), 924-937 (2021)
DOI: 10.1007/s11814-021-0743-2

pISSN: 0256-1115
eISSN: 1975-7220

Flow pattern study, gas hold-up and gas liquid mass transfer correlations in a bubble column: Effect of non - coalescing water - organic mixtures

Amina Fadili and Abdel Hafid Essadki†

Department of Chemical Engineering, Laboratory of Process Engineering and Environment,
Ecole Supérieure de Technologie, Hassan II University of Casablanca, Morocco
(*Received 15 July 2020 • Revised 21 January 2021 • Accepted 26 January 2021*)

Abstract−Experiments of hydrodynamic and gas liquid mass transfer were carried out in a bubble column of 19.4 cm internal diameter and of 4 m height. The liquid phase can be either tap water or a coalescence inhibitor system, using aqueous solutions of three alcohols (ethanol, 2-propanol and 1-butanol) with a volumetric concentration of 0.05% v/v and sodium dodecyl sulfate: SDS (10^{-3} mol/L) as an anionic surfactant. The hydrodynamic study involved placing wall pressure sensors in different axial positions of a bubble column to determine the gas hold-up in different regions and the influence of non-coalescing system on its evolution. The overall liquid movement induced by bubbles and the residence time distribution analysis of liquid phase was performed by using inductivity sensors. Gas hold-up results showed that the presence of the gas is more important in the zone far enough to the gas distributor (zone II). The results of the volumetric mass transfer coefficient (K_La) revealed that K_La decreased with the addition of alcohol, especially when the number of carbons in alcohol increased. K_La decreased more with the addition of anionic surfactant. It was also proven that a decrease in K_La was due to a decrease in K_L, which was due to a decrease of bubble rise velocity as well as of the diffusivity when alcohol or ionic surfactant was added. Correlations were developed linking gas hold-up and gas-liquid mass transfer coefficient to superficial gas velocity and surface tension gradient.

Keywords: Gas Hold-up Correlations, K_La Correlations, RTD, Semi Pilot Bubble Column, Coalescence-inhibiting System, Gas - Liquid Mass Transfer

INTRODUCTION

A variety of industrial gas-liquid reactions are performed in bubble columns. The mass transfer phenomena are intimately related to hydrodynamic and flow regimes. Thus, gas liquid transfer coefficient is related to the bubbles' characteristics, the turbulence and behavior of the bubble reactor as CSTR or plug with dispersion reactors. Because of the complexity and the interaction of many parameters in the hydrodynamics, the experimental approach, which consists of the determination of global, local gas hold-ups and flow regimes, is still used. The computational fluid dynamic (CFD) [1,2] approach gives local information but does not cover all aspects of a bubble column, and a unified theory is not yet developed to predict local gas hold-up. That is why experimental measurements are needed to give more data. Experimental data concerning global and local gas hold-ups are abundantly available in the literature. Several methods of measurements have been used. The basic one is volume expansion [3]. Manometric methods have also been plentifully employed [3-5]. More sophisticated methods have been carried out in bubble columns using γ-ray [6].

The behavior of bubbles in bubble columns is influenced by the physicochemical properties of the liquid (density, viscosity, surface tension, solute concentration, etc). The flow regime and gas hold-up in the presence of alcohols and electrolytes surfactants [7] in a non-uniformly aerated bubble column have been studied by Cachaza et al. [8], who concluded that for both types of surfactants, gas hold-up increases with the surfactant concentration. De Guido and Pellegrini [9] proposed a correlation representing the experimental data based on the dynamic surface tension theory applied in the entire range of gas superficial velocities (from 0.004 to 0.20 m/s), using different adaptive parameters.

Besani and Inzoli [10] studied the effect of liquid phase properties on bubble column fluid dynamics by using tap water, aqueous solutions of NaCl, water-ethanol mixture, and solutions of water-monoethylene glycol of different concentrations. Gas hold-up measurements were used to investigate the global fluid dynamics, the flow regime transition, and the foaming phenomena. Correlations were proposed to estimate bubble shape and interfacial area, for the different liquid phases tested. These correlations were based on the gas hold-up measurements, which were determined by the volume expansion.

Mass transfer is another aspect concerning the design and scale-up in bubble column. Gas liquid mass transfer remains a subject of discussion because the estimation of volumetric mass transfer coefficient (K_La) is very sensitive to different parameters, such as the position of the probe, hydrodynamic conditions, and the probe dynamic [11-13]. Although the estimation of K_La is abundant in literature, the accuracy of the estimated value of K_La should be analyzed. This aspect concerns the response of probe, the local hydrodynamic, the bubbling characteristics, turbulence, and the presence of surfactants. Mariano et al. [14] studied the mass transfer mechanism and the shape of a single growing bubble. They concluded

†To whom correspondence should be addressed.
E-mail: essadkiha@gmail.com

that the liquid viscosity and the surface tension increase the Sherwood number ($Sh=K_L \cdot d_B/D_L$; K_L: liquid-side mass transfer coefficient, d_B: bubble diameter, D_L: molecular diffusion of oxygen in liquid), while the liquid density reduces it. The effects of the addition of different types of surfactants to air-water system on gas hold-up and mass transfer were studied by Ramazan et al. [15] in a co-current downflow contacting column. The study revealed that the values of gas hold-up in the air-surfactant solution system were larger than the ones in the air-water system. Furthermore, the values of the volumetric mass transfer coefficient in the air-surfactant solution system were lower than the ones in the air-water system. Even the specific gas-liquid interfacial area (a) increased with the addition of surfactant. Kovats et al. [16] studied the influence of viscosity and surface tension on bubble dynamic and gas liquid mass transfer. They concluded that with decreasing the surface tension and the viscosity, the bubble size is diminished, but neither the addition of glycerol nor the addition of surfactant was found to be beneficial to mass transfer from the CO_2 bubbles into the liquid. A recent review [17] presented the current understanding of the multiscale multiphase phenomena inside bubble column reactors (BCRs). Some progress is still needed to better understand and predict the effect of the liquid nature, especially the water-alcohol mixture.

As the bubble column used is large diameter and large-scale (4 m in height, inner diameter of 0.19 m), the gas hold-up should be investigated in different regions of it. In addition, conductivity signals are used to give complementary information about the influence of bubbling in the flow pattern. These hydrodynamic studies can better explain the results obtained in the gas liquid mass transfer using the water-alcohol mixture (ethanol, propanol and butanol) or SDS as anionic surfactant.

Aqueous solutions of alcohols having a short carbon chain such as ethanol, propanol, and butanol are of great importance because of their typical physicochemical properties in many compositions [18]. This study is devoted to examining the effect of surfactants on gas liquid mass transfer. The alcohols used behave as surfactants, SDS is an anionic surfactant. Most of the papers have focused on one type of alcohol or surfactant.

In the present study, the density and viscosity are not affected by the addition of minute alcohol or ionic surfactant with low concentration; only the effect of surface tension can play a role in hydrodynamics and mass transfer. The range of the surface tension used in this work, varying between 0.064 and 0.072 N/m, is not large enough, whereas the surface tension gradient is relatively wide and varies between 0.23 and 418 N/m. Guo et al. [19] studied the behavior of bubbles in terms of the gas hold-up in a bubble column with pure liquids and ethanol and n-butanol solutions. These researchers used the concept of dynamic surface tension in which the surface tension gradient plays a great role to explain their results. An algebraic criterion was used [19] to predict the critical concentration at which the maximum gas hold-up occurred and the maximum frothing ability occurred at the composition for which this criterion $\theta(x)(d\sigma/dx)^2$ reached its maximum, where x is the mole fraction of alcohol, $\theta(x)=x(1-x)/(1-x+kx)$, $k=V_1/V_2$, and V_1 and V_2 were the molar volume of ethanol and water.

This distinct difference of bubble behavior was attributed to the dynamic surface tension effect in the alcohol solutions, which inhibited bubble coalescence. The latter depended on the type of alcohol and was more inhibited by alcohols with longer carbon chains. Syeda et al. [20] also studied the effect of alcohols on the gas hold-up in a bubble column and successfully predicted the trend in variation of the gas hold-up using the dynamic surface tension theory. The concept of this theory was adopted in our study by extending the study for three types of alcohols and an anionic surfactant both for hydrodynamics and for the gas liquid mass transfer. The proposed correlations will introduce the surface tension gradient rather than the bulk surface tension.

EXPERIMENTAL SETUP AND METHODS

Experiments were carried out in a cylindrical semi-batch bubble column (batch liquid phase) made of plexiglass of 19.4 cm internal diameter and 4 m height. The gas phase (air) is dispersed through a multiple-orifice nozzle at the bottom of the column by a distributor provided with multi-orifice 32 holes of 1 mm in diameter uniformly distributed over its surface. Fig. 1(a) shows a schematic diagram of the bubble column used in this study. The gas flow is controlled by a Brooks flow meter (Model 1355) previously calibrated which ensures a superficial velocity between 0.56 and 9.7 cm/s. A manometer was placed underneath the gas distributor to measure the pressure drop versus the gas flow-rate in order to correct the calibration.

The liquid phase can be either tap water or non-coalescing water - alcohol mixtures (0.05% v/v). The alcohol mixed with the water is either ethanol, 2-propanol or 1-butanol. Sodium dodecyl sulfate (SDS) (10^{-3} mol/L) was also used as an anionic surfactant.

A hydrodynamic study was conducted by placing the wall pressure sensors and conductivity probes in different axial positions of the bubble column to determine the gas hold-up in different regions. The height of the liquid in the bubble column is 2 m.

Wall pressure sensors were placed in different axial positions of the bubble column to measure gas hold-up locally, for a region covering a height of 0.75 m and the overall gas hold-up covering a height of 150 cm. The differential pressure was measured by two consecutive resistive sensors membrane pressure (Keller, PR25) that offers ±0.2% full-scale accuracy for the range 0-500 mbar (Fig. 1(d)). The column was then progressively filled with water. For each water depth (25 cm), the current was noted. The calibration was repeated systematically after a series of manipulations to check the reproducibility of the calibration. For each pressure sensor, the calibration curves exhibit a linear relationship between static pressure and signal (current). Then, the sensors were connected to the acquisition system (Fig. 1(b)). The three membrane pressure sensors as piezoresistive transmitters (Keller PR25) were placed in different axial positions at 0.25 m, 1 m and 1.75 m from the gas distributor. The signals collected are electric currents.

A circuit board (Fig. 1(c)) was designed to power the sensors with generators (PWR1, PWR2, PWR3) as well as to connect them with the acquisition board (CI0, CI1 and CI2). The three signals were then collected (SEN1, SEN2, SEN3) for statistical and signal analysis with appropriate acquisition frequency. An ADLINK USB-1903 16-bit A/D (Fig. 1(b)) acquisition card with eight current-input differential channels was used.

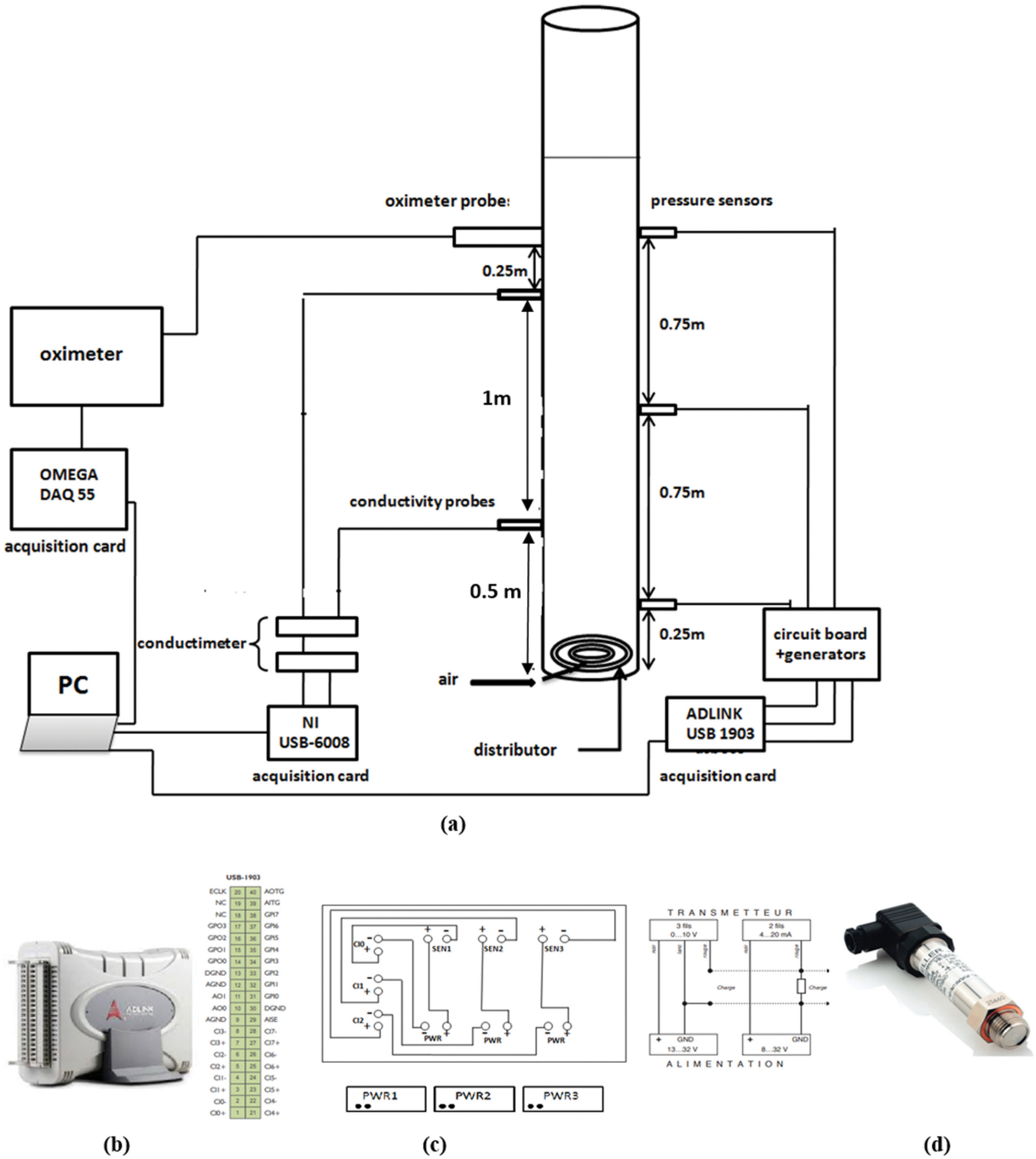

Fig. 1. Experimental apparatus: (a) Schematic diagram of the bubble column for ε_g, RTD and K_La measurements. (b) Acquisition card. (c) Circuit board. (d) Piezoresistive transmitters (Keller PR25).

Two conductivity probes (Tacussel) were used, placed in two positions at, respectively, 0.5 m and 1.5 m from the gas distributor. The corresponding conductivity meters were two CD 810 having differential outputs to acquire three analog voltage signals. The digitized signals were ensured by using an Analog/Digital acquisition board: A USB-6008 acquisition board that has eight analog inputs (12 bits, 10 ks/s) and two analog outputs (150 Hz). It has analog I/O, digital I/O and a 32-bit counter.

Preliminary experiments revealed that the best results of gas hold-up were obtained when the distance between two pressure sensors was greater than 50 cm. Three pressure sensors were installed axially at heights of 25, 100 and 175 cm above the distributor, respectively. The distance between two consecutive sensors was 75 cm. The overall gas hold-up covered a region of 150 cm as height (sensors 1 and 3). Two other gas hold-ups were also measured covering two axial zones: zone I (sensors 1 and 2) covering one meter above the gas distributor, and zone II (sensors 2 and 3) covering the distance greater than one meter above the gas distributor.

In general, in the bubble columns, the pressure drop by friction was negligible and with $\rho_g << \rho_l$ (density of gas is negligible com-

Table 1. Surface tension of studied solutions at T=20 °C

System	Surface tension (mN/m)
Water	71.9
Ethanol 0.05%	71.94
2-Propanol 0.05%	68.3
1-Butanol 0.05%	67.7
SDS (10^{-3}) M	64

pared to that of liquid), the gas hold-up can be deduced by the following expression [4,11]:

$$\varepsilon_g = 1 - \frac{\Delta p}{\rho_l g \Delta h} \quad (1)$$

where Δp is the differential static pressure between two sensors placed at a distance Δh.

A certain amount of alcohol (ethanol, propanol or butanol) covering a volume concentration of 0.05% (v/v) or SDS with 10^{-3} M concentration was introduced into the bubble column by syringe. Water was added gradually until it reached a height of 2 m. To better mix alcohol with water, the gas was introduced.

Solutions with alcohol and SDS are characterized by the surface tension. The addition of these alcohols or SDS with a relatively low concentration does not affect the viscosity of the solution. Table 1 gives values of the surface tension of the solutions used, which was measured by using the ring method (Kruss tensiometer).

Gas - Liquid Mass Transfer Measurement

The dissolved oxygen concentration was measured using probe oximetry (CellOx 325) at 1.75 m from the gas distributor (Fig. 1). The measurements of the oxygen gas concentration were recorded using a data acquisition system connected to a PC. The signals obtained by the data acquisition card were converted into the concentration and stored in files. Calibration was performed by saturating the liquid oxygen column by compressed air. The concentration was then adjusted to read the saturation value for the gas temperature to the measured ambient atmospheric pressure. This theoretical concentration is given by the French standard (AFNOR) T 90 032 for the solubility of oxygen in water. The technique of de-oxygenation - reoxygenation is used to determine the volumetric gas liquid mass transfer coefficient. Oxygen is removed by introducing sodium sulfite (Na_2SO_3) in the presence of a catalyst in solution (Co^{2+}).

RESULTS AND DISCUSSION

1. Effect of Alcohol Type Solution, Anionic Surfactant and Axial Zone on Gas Hold-up

The gas hold-up by zone was performed using two consecutive sensors in a distance covering 75 cm. Two distinguished regions were under study: the first one (zone I) covered 1 m above the gas distributor; the second region covered a distance between 1 and 2 m above the gas distributor (Fig. 1(a)). The gas hold-up covering zone I and zone II was, respectively, denoted as ε_{12}, and ε_{23}, whereas the global hold-up covering the two zones was denoted as ε_{13} or ε_g.

Fig. 2 shows that the value of gas hold-up for aqueous 0.05% 1-butanol solutions is less in zones close to the sparger than in zones far enough to the gas sparger. The difference between gas hold-ups in the two zones becomes larger as the superficial gas velocity

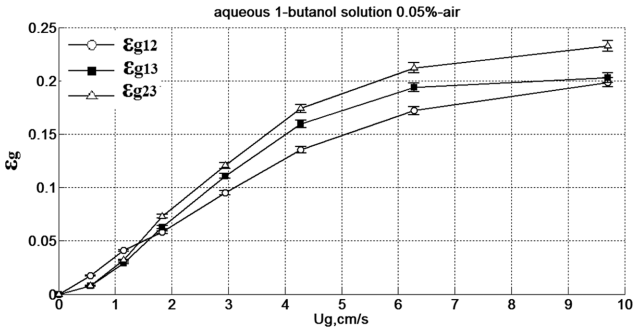

Fig. 2. Evolution of gas holdup for zones I, II and global gas holdup for 1-butanol 0.05% aqueous solution.

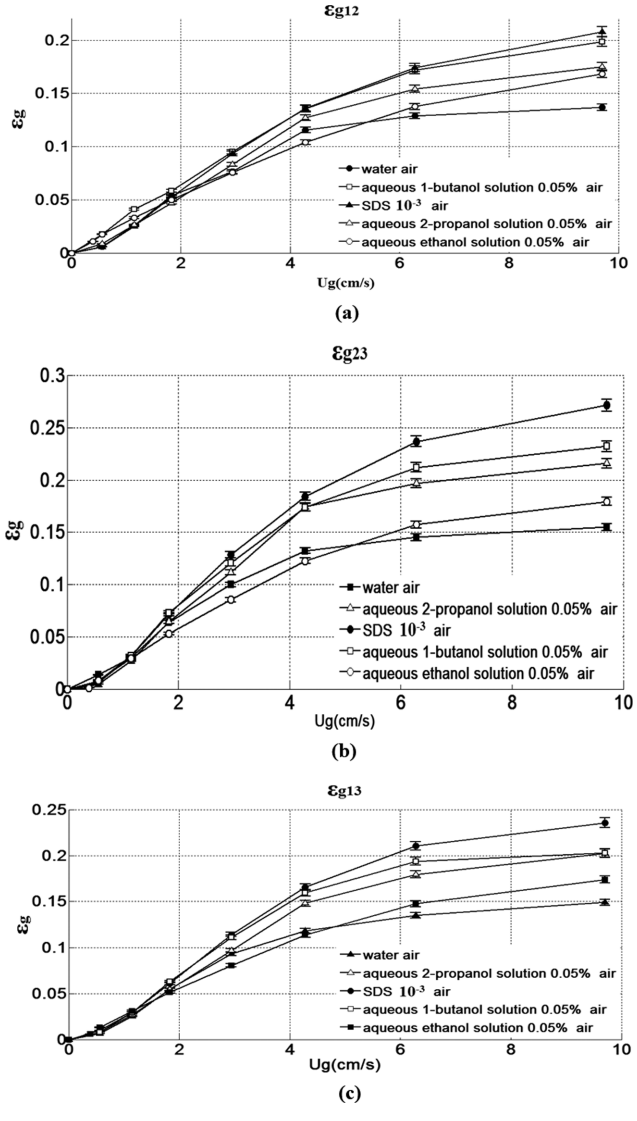

Fig. 3. Comparison of gas holdup for zones I and II and global gas holdup for pure water, water-alcohol mixture solutions and SDS solution.

increases. As expected, the global gas hold-up shown in Fig. 2, measured between the sensors 1 and 3, takes the average values with respect to the gas hold-ups measured in zones I and II. The same tendency was obtained with alcohol solution or with pure water-air system.

Fig. 3(a) presents the evolution of gas hold-up in zone I versus superficial velocity for a different type of alcohols and SDS as inhibiting system promoting bubble break up. The gas hold-up increases with the number of carbons in the alcohol. The influence of SDS solution is similar to butanol solution. The difference in gas hold-up between different types of alcohol increases with increasing gas velocity. In zone II as presented in Fig. 3(b), the difference in gas hold-up between SDS solution and alcohol solution is more pronounced. In general, the global gas hold-up (ε_{13}) is more important by using an anionic surfactant (SDS) comparatively to alcohol solutions. The gas hold-up increases also with the carbon number in the alcohol increases (ethanol, propanol and butanol) as observed in Fig. 3(c).

2. Interpretation of the Gas Hold-up Results

The increase in gas hold-up by the addition of alcohols or ionic surfactant is mainly due to a reduction of the bubble-rise velocity caused by the bubble size reduction [21]. Thus, in the case of small bubbles in surfactant solutions, the addition of surfactants affects the internal bubble circulation so that the bubbles can be assimilated into solid spheres. Surfactants increase the surface rigidity as a consequence of dynamic surface tension, by covering part of the bubble surface allowing an increase of bubble drag coefficient similar to a rigid sphere. This diminishes the terminal velocity [22]. In fact, the coalescence inhibition mechanism is responsible for the bubble size reduction. In general, the coalescence rate can be modeled by the physical film drainage in which three steps allow the bubble coalescence: a collision between two bubbles trapping a liquid film, drainage of the liquid film, and a film rupture and coalescence [23]. The coalescence inhibition can be operated by the adsorption of surface-active solutes at bubble/solution interface via two different means, steric hindrance and electrostatic repulsion, if the surface-active solutes are charged.

Steric hindrance effect is the principal mechanism operating when the solutes are uncharged, such as with alcohol. Oolman and Blanch [24] and Zahradnik et al. [25] reported that the bubble coalescence in aqueous alcohol solutions is significantly hindered and that longer chain alcohols inhibit bubble coalescence more effectively. The addition of minute quantities of aliphatic alcohol molecules in water leads to the inhibition of coalescence phenomena by adsorption. Due to the hydrophobic and hydrophilic parts, a surface tension gradient force is created, allowing an immobilization of the gas-liquid interface. The coalescence is then hindered.

When the charged surface-active solutes (such as ionic surfactants) are present, their adsorption will usually determine the overall charge on the bubble/solution interface. The charges on the bubble surface influence the distribution of ions in the liquid surrounding it, where counter-ions are attracted and co-ions are repelled. This gives rise to an unequal distribution of electrical charges across the interface forming the electrical double layer. Stern model describes two regions: an inner region of strongly held counter-ions (the Stern layer) and a diffuse region where ions (both counter-ions and co-ions) are distributed according to electrical potential and Brownian motion (the diffuse layer). The Stern plane is located one hydrated ion radius away from the charged surface.

The non-polar tails of SDS, as an anionic surfactant, experience repulsion with polar water molecules. The tails are pushed to the gas media. An equilibrium state is then reached to reduce the interfacial area between water and tails to a minimum [26].

The internal circulation, together with the external liquid-to-surface shear, contributes to the accumulation of surfactants on the rear of the bubble, which is referred to as a stagnant cap [27]. Boussinesq [28] first proposed that the reduction in internal circulation in gas bubbles and in the drops is due to the interfacial accumulation of contaminants organized as a monolayer, which was validated experimentally [29]. The gas hold-up results (Fig. 2 and Fig. 3) show also that the presence of the gas is more important in the zone far enough from the gas distributor (zone II). This aspect can be explained in light of the rear stagnant cap (RSC) theory [30]. This theory explains that an adsorption process proceeds and leads to the formation of RSC. During the bubble rise, the rear cap is increasingly filled with surfactants. In the zone far enough to the sparger, the RSC is larger than in the zone close to the sparger allowing for a retardation of the rising velocity. The bubble stabilization due to the surfactant allows gas bubbles to exist at the top of the liquid. This explains the difference on gas hold-up between zone I and zone II.

The addition of ethanol, 2-propanol or 1-butanol with a volumetric concentration of 0.05% v/v corresponds to low molar fraction (x) (x=0.000195 for ethanol, x=0.000149 for 2-propanol and x=0.00012 for 1-butanol). One mM/L of SDS corresponds to $x=1.8\ 10^{-5}$ as a molar fraction.

With this low molar fraction, the surface tension decreases from 71.9 to 64 mN/m at 20 °C. The decrease in the surface tension is not sufficient to explain the discrepancies in the gas hold-up.

Guo et al. [19] found that the dynamic surface tension strongly affects the bubble behavior. The dynamic surface tension model was proposed by Andrew (1960) to explain the bubble behavior in the alcohol-water mixture [19].

The criterion $Cr(x) = \theta(x)(d\sigma/dx)^2$ is used to quantify the coalescence inhibition.

where x is the mole fraction of alcohol, $\theta(x)=x(1-x)/(1-x+kx)$, $k=V_1/V_2$, and V_1 and V_2 are the molar volume of alcohol and water.

Syeda et al. [31] demonstrated that the concentration at which maximum value of $C(d\sigma/dx)^2$, i.e., (concentration×surface tension gradient with respect to concentration^2) is obtained corresponds to the concentration at which maximum gas hold-up enhancement occurs. They used four electrolytes, namely, NaCl, $MgSO_4{\cdot}7H_2O$, Na_2SO_4 and $CaCl_2{\cdot}2H_2O$, and the concentrations of the solutions were varied from 0 to 0.3 mol/l.

This criterion was adopted to expand the study for ethanol, propanol, butanol, and SDS. We are interested in the values of this criterion obtained for the mole fractions used in this study. The higher these values, the more effectively the inhibition of coalescence occurs. As suggested by Guo et al. [19], this criterion also predicts the critical concentration at which the maximum gas hold-

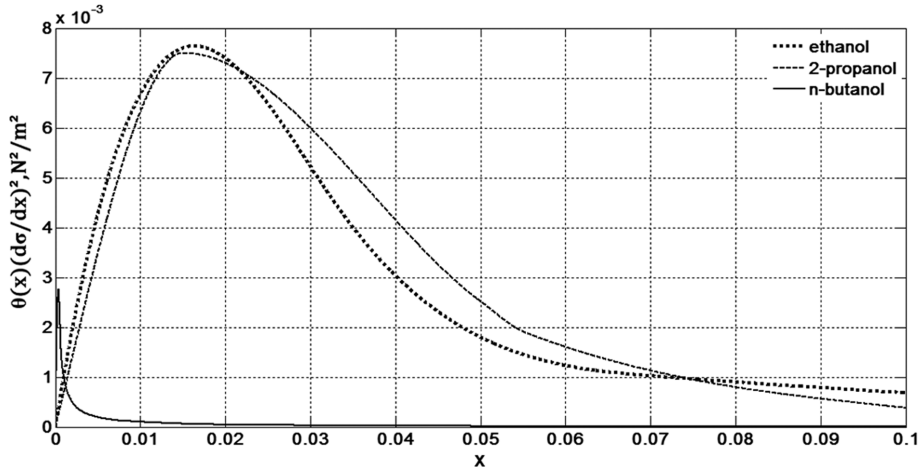

Fig. 4. Effect of alcohol molar fraction on inhibition of bubble coalescence.

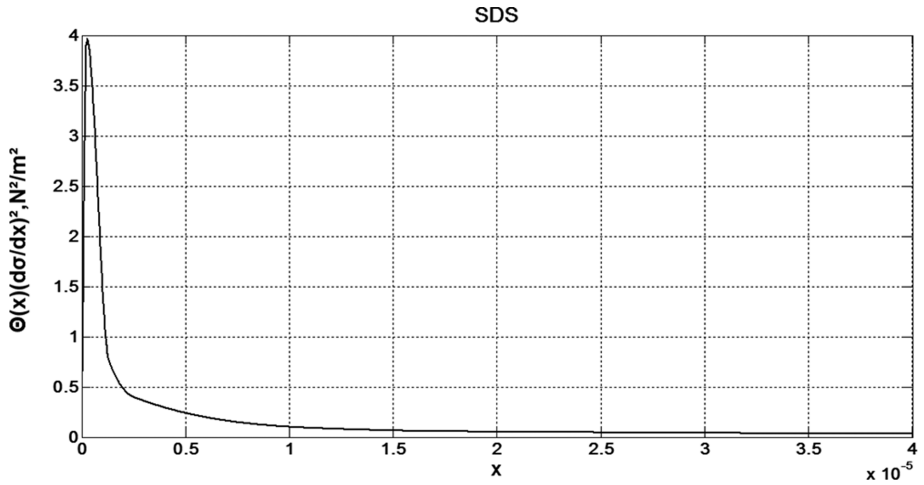

Fig. 5. Effect of SDS molar fraction on inhibition of bubble coalescence.

up occurred. According to this criterion, the maximum frothing ability occurred at the composition for which $Cr(x)=\theta(x)(d\sigma/dx)^2$ reached its maximum.

From the data of the surface tension of ethanol, 2-propanol, 1-butanol, and SDS as a function of the molar fraction: $\sigma(x)$ available in the literature [32-35], a program was developed (Matlab) to interpolate the low values of σ to obtain accurate values of surface tension gradient ($d\sigma/dx$) in low molar fraction. The criterion of coalescence inhibition ($\theta(x)(d\sigma/dx)^2$) was then deduced. Figs. 4 and 5 show the curves of the criterion, respectively, for alcohols and SDS. Because of the high values of the surface tension gradient of SDS, the values of the criterion are high relative to the alcohols.

The maximums obtained for ethanol and propanol are close and are approximately 0.0075 for molar fractions of 0.016 and 0.017, respectively, for ethanol and propanol. Whereas for butanol, this maximum is obtained for a relatively low molar fraction (x=0.001) because the surface tension of butanol decreases rapidly. From these curves, the values of the coalescence inhibition criterion were determined for each type of alcohol and for SDS. The values thus obtained are as follows:

Cr_{SDS} (x=1.8 10^{-5})=0.055>$Cr_{Butanol\text{-}1}$ (x=0.000121)
=0.0014>$Cr_{Propanol\text{-}2}$ (x=0.0001497)
=0.00101>$Cr_{Ethanol}$ (x=0.000195)=0.00021.

These values increase gradually when the number of carbons in the alcohol is increased (from ethanol to butanol). The value of the coalescence inhibition criterion is more important for the case of anionic surfactant (SDS) which presents a very high surface tension gradient compared to that of alcohols.

The increase in the coalescence inhibition criterion, which results in a reduction in the size of the bubbles by the bubble break-up phenomenon, explains in a remarkable way the increase in gas hold-up.

Data for the gas hold-up (ε_g) can be correlated to the superficial gas velocity and the surface tension gradient to highlight the effect of the dynamic surface tension. The recommended correlation for ε_g in semi pilot bubble column for both systems (air-water-alcohol mixture and SDS solution) is:

$$\varepsilon_g = 0.0221 U_g^{1.26} \left|\frac{d\sigma}{dx}\right|^{0.015} \quad (2)$$

Table 2. Correlation for 0.56 cm/s<U_g<6.3 cm/s: Global gas holdup ($d\sigma/dx$ is expressed in N/m)

Correlation	Standard deviation			
$\varepsilon_g = 0.0221 U_g^{1.26} \left\|\frac{d\sigma}{dx}\right\|^{0.015}$	Ethanol	Propan-2-ol solution 0.05%	Butan-1-ol solution 0.05%	SDS solution 10^{-3} mol/L
	24%	14.3%	14.2%	16%

In Table 2, the standard deviation of this correlation is also presented to show the accuracy degree of each system. U_g is expressed in cm/s (0.56 cm/s<U_g<9 cm/s) and $d\sigma/dx$ is expressed in N/m. This correlation can be used for a molar fraction (x) ranging from 0 to x_{max}, where x_{max} corresponds to the maximum of Cr(x).

The surface tension gradients of alcohols and SDS used in this study are:

$$\left(\frac{d\sigma}{dx}\right)_{Ethanol} (0.000197) = 0.228 \text{ N/m};$$

$$\left(\frac{d\sigma}{dx}\right)_{Propanol\text{-}2} (0.000149) = 1.82 \text{ N/m};$$

$$\left(\frac{d\sigma}{dx}\right)_{Butanol\text{-}1} (0.000121) = 4.25 \text{ N/m};$$

$$\left(\frac{d\sigma}{dx}\right)_{SDS} (1.8 \ \ 10^{-5}) = 418.6 \text{ N/m}$$

For relatively high superficial gas velocity (greater than 6.3 cm/s), the predominance of the macro scale turbulence effect reduces the role of the surface tension [4,36,37]. However, the proposed correlation covering the homogeneous and heterogeneous flow can be accepted, as the standard deviation is relatively low (not exceeding 24%).

3. Tracking and Residence Time Distribution (RTD)

Phase liquid tracking was carried out, as is the case with the batch liquid phase, to evaluate the overall liquid movement induced by bubbles. Yet, a residence time distribution (RTD) analysis of liquid phase was performed for a relatively weak liquid flow-rate in order to determine the influence of different types of bubbling on the model of the liquid flow.

The hydrodynamic characteristics of the liquid are influenced by the gas flow rate and the nature of the bubbling. The tracing technique is one of the techniques that can be used to determine the circulation velocity of the liquid, induced by the gas while considering that the momentum of the liquid must be conserved.

In the continuous mode in which the liquid is in motion, the RTD becomes highly effective in quantifying the flow of the liquid. It consists of performing "stimulation" or "excitation" without disturbing the system at the reactor inlet and of recording the response to the output. The analysis of this response enables the description of the real behavior of the reactor, by comparison with theoretical models, which are developed from models of ideal flows. The results can be exploited for a better modeling of the gas - liquid mass transfer in which the transfer coefficient K_La is an identified and unmeasured quantity. As a result, the flow model influences the accuracy of K_La values. The conductivity probes set up axially in the bubble column section are used to record the tracer concentration resulting from the injection of 60 mL of a saturated KCl solution. The output is considered by the probe placed at 1.5 m above the distributor.

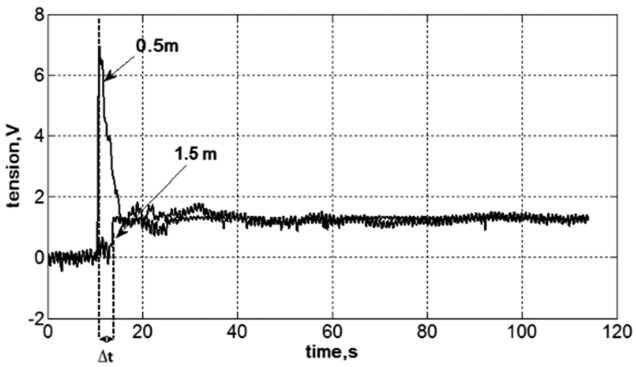

Fig. 6. Conductivity signal for pure-water-air system at superficial gas velocity of 0.56 cm/s.

3-1. Tracking for Batch Mode

Water-air, alcohol-air, and SDS solutions are used. The superficial velocity of the gas varies between 0.056 cm/s and 9.7 cm/s. A sample of the signals obtained is presented in Fig. 6 showing the effect of low gas velocity (0.56 cm/s) for the water-air system. A peak has clearly appeared for the first probe that is closer to the injection point, whereas the signal of the second probe is amortized because of the dilution of the tracer. However, these signals could be used to measure the velocity of the liquid by calculating the variation Δt, knowing the distance between the two conductiv-

Table 3. Effect of superficial gas velocity on the induced liquid velocity for the water - air system and coalescence inhibitor system

U_g (cm/s)	U_L (cm/s): air-water	U_L (cm/s): Ethanol (0.05%)	U_L (cm/s): Propanol (0.05%)	U_L (cm/s): Butanol (0.05%)	U_L (cm/s) SDS 10^{-3} M
0.56	0.16	0.11	0.1	0.1	0.1
2.9	0.71	0.7	0.35	0.29	0.25
9.7	1.25	1.25	1.2	0.83	0.7

ity probes. The same trend is obtained for coalescence inhibitor system (not presented) as for the water-air system. Table 3 shows the influence of gas velocity on the induced liquid velocity for the water-air system, and coalescence inhibitor system. It is noted that liquid velocity increases with the superficial gas velocity, and that for a fixed gas velocity the average liquid velocity decreases as carbon number of the alcohol increases (from ethanol to butanol). The decrease of liquid velocity is more pronounced for SDS solution.

3-2. Residence Time Distribution (RTD) Measurement for Continuous Mode

The liquid RTD was also determined by means of the tracer response technique. Using a low liquid flow rate of 0.27 L/s and a liquid height of 2.15 m, a solution of 3 M KCl was injected at the same injection point as for the batch case (0.5 m from the gas distributor).

The probe to measure conductivity had previously been calibrated so that the tracer concentration could be determined from the recorded conductivity profile.

To obtain the E(t) curve from the C(t) curve, we divided C(t) by the integral:

$$E_{exp}(t)=\frac{C_{KCl}(t)}{\int_0^{\infty} C_{KCl}(t)dt} \tag{3}$$

The two characteristic quantities of the distribution, the average (or mean residence time) and the variance (moment 1 and 2 of the distribution) are determined by E(t):

$$\text{Mean residence time: } \tau=\mu=\int t\ E(t)\ dt=\Sigma t\ E(t)\Delta t \tag{4}$$

$$\text{Variance: } \sigma_t^2=\int(t-\mu)^2\ E(t)\ dt=\Sigma t^2\ E(t)\Delta t-\mu^2 \tag{5}$$

The reduced variance is calculated by the equation:

$$\sigma^2=\frac{\sigma_t^2}{\mu^2} \tag{6}$$

The piston model with axial dispersion was used to characterize the flows in the bubble column. The differential equation representing the axial dispersion of a tracer is:

$$\frac{\partial C}{\partial t}+U\frac{\partial C}{\partial z}=D\frac{\partial^2 C}{\partial z^2} \tag{7}$$

D is the axial dispersion.

The analytical solution of such an equation [38], considering the boundary conditions and the fact that our experiment will be considered with "Open Vessel", i.e., in z=0 and in the measured point z=L the flow is open to dispersion, is expressed as:

$$E(\theta)=\frac{1}{2}\sqrt{\frac{Pe}{\pi\theta}}\exp\left[-\frac{Pe(1-\theta)^2}{4\theta}\right],\ \theta=t/\tau \tag{8}$$

in which Pe=U L/D is the Peclet number, D is the axial dispersion, U is the liquid velocity, L is the length of the considered zone of the bubble column considered as studied system and τ is the mean residence time. Peclet number can also be determined by using the reduced variance:

$$\sigma=\frac{2}{Pe}+\frac{8}{Pe^2} \tag{9}$$

The tank-in-series model can be also used consisting of N reactors perfectly mixed. The solution giving E(t) curve is:

$$E(t)=\left(\frac{N}{\tau}\right)^N\frac{t^{N-1}}{(N-1)!}\exp\left[-N\frac{t}{\tau}\right] \tag{10}$$

The correspondence between the two models can be used:

$$Pe=2(N-1)\text{ or }N=\frac{Pe}{2}+1 \tag{11}$$

Experimental data have been fitted to the proposed models using a direct method (simplex) to obtain the unknown model parameters. MATLAB 7 (The MathWorks, USA) was chosen as the programming language. MS Excel was also used, as well as the least square method. This approach was adopted in the previous work [39]. The signal recorded by the closest probe to the injection point show that this signal is not a real Dirac δ-pulse signal. The real curve E(t) was obtained by using two signals and by the convolution-deconvolution method. To overcome the injection and detection methods, two measurements of two-level concentrations can be made in the reactor: x (t) and y (t). If both functions are normalized:

$$\int_0^{\infty}x(t)\ dt=\int_0^{\infty}y(t)\ dt=1 \tag{12}$$

The outlet signal y(t) is a convolution of x(t) and E(t): y = x*E:

$$y(t_2)=\int_0^{t_2}x(t_1)\ E(t_2-t_1)dt_1 \tag{13}$$

If the system is linear, we can apply the Laplace transform L(p) to x (t) and y (t) to obtain X (p) and Y (p). Thus,

$$Y(p)=X(p)\cdot G(p);$$

$$G(p)=\int_0^{\infty}\exp(-pt)\ E(t)dt \tag{14}$$

The fast Fourier transform FFT [39], can be also used to obtain E(t):

$$E(t)=IFFT\left(\frac{FFT(y(t))}{FFT(x(t))}\right) \tag{15}$$

IFFT is the inverse FFT.

Thus, we could identify all the parameters with good estimation by fitting the models on E(t) instead of y(t). The inlet (position 0.5 m above the gas distributor) and outlet signals (1.5 m above the gas distributor) were recorded. Figs. 7(a) and 7(b) show that the signals obtained for gas velocity of 0.56 cm/s and 1.83 cm/s are disturbed by the passage of bubbles. That is why a smoothing program was developed for a better modeling of the liquid flow. Fig. 8 shows the signals obtained after the smoothing. The smoothing signals are then normalized.

Experiments conducted for water-alcohol and water-SDS systems proved that the bubble column behaves as a perfect mixed reactor in all studied superficial gas velocity in which Peclet number is between 1 and 4. This result is important for gas liquid mass transfer because the perfect mixing model could be applied. Even with relatively low superficial gas velocity, the model fits the experiment with a Peclet number equal to 1.

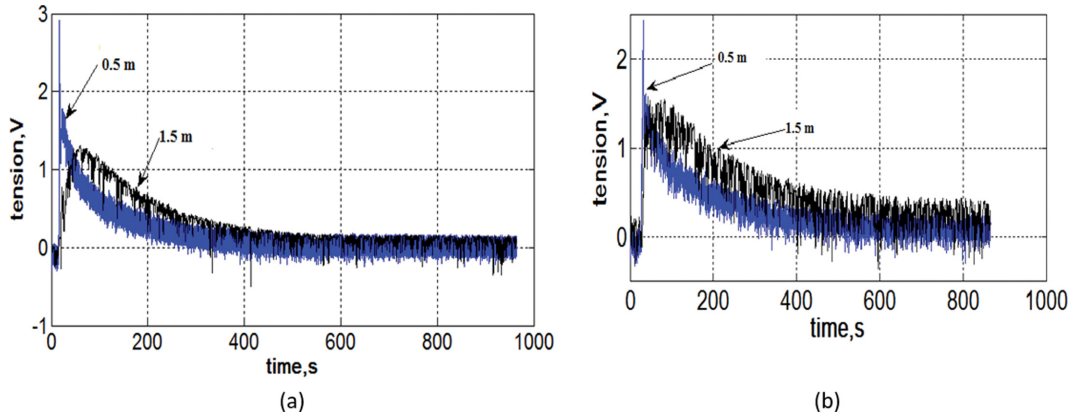

Fig. 7. Conductivity signals (Volt): Inlet signal (position 0.5 m), Outlet signal (position 1.5 m). (a): U_g=0.56 cm/s; (b): U_g=1.83 cm/s.

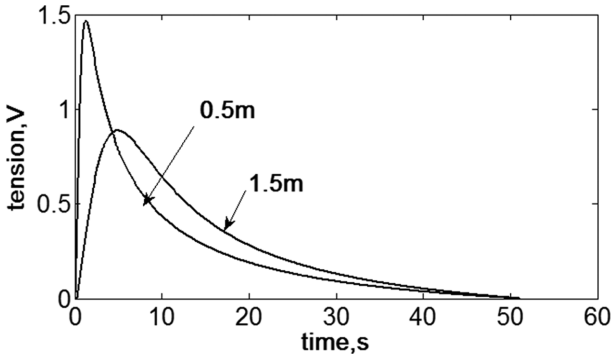

Fig. 8. Smoothed conductivity signals (Volt): Inlet signal (position 0.5 m), Outlet signals (position 1.5 m). U_g=1.83 cm/s.

4. Gas - Liquid Mass Transfer

Volumetric mass transfer coefficients (K_La) were measured in tap water, alcohol-water mixture solutions (0.05% v/v), and SDS solution (10^{-3} M) as a coalescence-inhibiting system. Deoxygenation and Reoxygenation method was applied. The oxygene is removed by introducing 20 g sodium sulfite (Na_2SO_3) in the presence of cobalt ($[Co^{2+}]$=0.5 mg/L) as a catalyst:

$$Na_2SO_3 + \frac{1}{2}O_2 \xrightarrow{Co^{++}} Na_2SO_4$$

Fig. 9 shows the stages of deoxygenation and reoxygenation.

After each experiment, the solution is renewed and therefore replaced by a fresh solution.

Even the gas liquid mass transfer is measured for a liquid batch mode. The results of RTD measurement for low liquid velocity can be used for batch mode to come up with the conclusion that the mixing is perfect in bubble column. In this case, the perfectly mixed reactor assumption is valid. Hence, the concentration evolution of oxygen is governed by the following equation:

$$\frac{dC_L}{dt} = K_La(C_L^* - C_L) \tag{16}$$

C_L^*: saturation concentration of oxygen in the liquid phase (kg/m^3).

The global mass transfer coefficient K_La was evaluated by experiment. The probe dynamics was taken into account. The preliminary experiment was used to determine the time constant (τ= 1/K_p) [11]. The dynamics of the probe relative to the actual concentration (C_L) in the liquid was modeled by a first-order response which takes into account the delay:

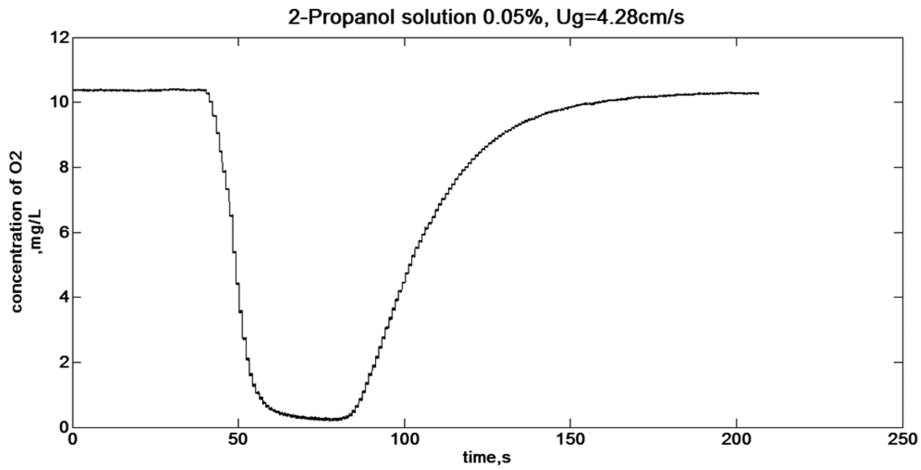

Fig. 9. Desoxygenation and reoxygenation stages.

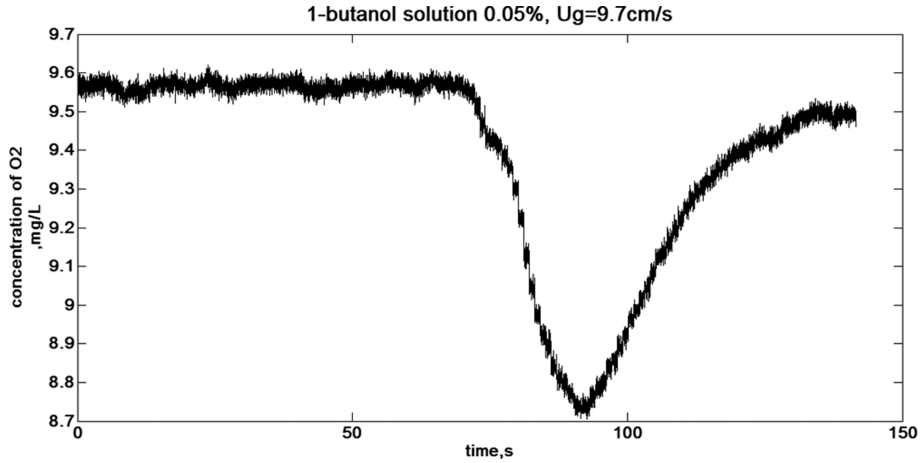

Fig. 10. Fluctuations of de-oxygenation and reoxygenation curve indicating the perturbation of foam.

$$\frac{dC_P}{dt} = K_p(C_L - C_P) \tag{17}$$

C_P: is the concentration measured by the probe with delay. The first-order differential equation describes the response dynamic of the probe during the re-oxygenation of the medium. Eqs. (16) and (17) are two-coupled differential ones. To transform these differential equations to algebraic ones, the Laplace transform is used with the initial conditions $C_L=C_P=C_0$ at t=0. In general, C_0 is different from zero, especially in the case of high superficial gas velocities. In most articles of the literature, C_0 is taken equal to zero, which can induce an error for the identification of K_La.

The inverse Laplace is then used to evaluate the measured concentration (C_p(t)). The obtained result is described by the following relation:

$$C_p(t) = C^*\left\{1-\left[\frac{1}{T_1-T_2}\right][T_1 e^{-K_L a.t} - T_2 e^{-Kp.t}]\right\} + \frac{K_p C_L(0)}{(K_L a - K_p)}[e^{-K_L a.t} - e^{-Kp.t}] + C_p(0)e^{-Kp.t} \tag{18}$$

The details of the calculation are presented in the appendix.

K_La was estimated by a parameter-fitting program using the optimization method from the code "fminsearch" contained in the mathematical tools of Matlab 7. The identification is deduced by fitting the simulated and experimental curves. For each experiment, temperature is considered. As mass transfer coefficients are influenced by temperature due to the effect of diffusivity, the measured K_La at temperature T is converted to K_La at 20 °C according to the following relation [40]:

$$K_L a\,(20\,^{\circ}C) = K_L a\,(T)\cdot\theta^{20-T} \tag{19}$$

The value of θ is estimated to 1.024

The presence of the foam for propanol and butanol and especially for SDS as anionic surfactant makes it difficult to measure K_La for high gas velocity, especially when the oxygen sensor is placed near the free surface. For high gas velocity, a high volume of foam is observed, especially for the butanol and SDS. This hinders the measurement of K_La. An example of deoxygenation - reoxygenation is shown in Fig. 10. The foam disturbance on the K_La measurement is negligible for gas velocity not exceeding 6.3 cm/s.

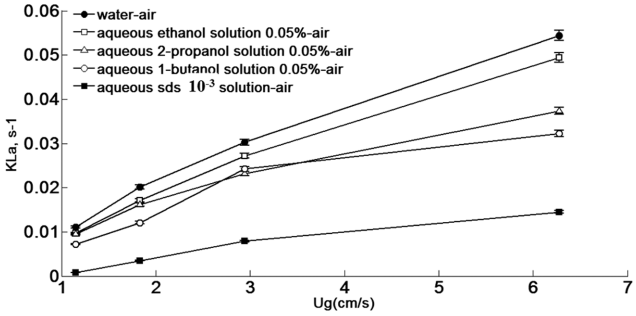

Fig. 11. Gas-liquid oxygen transfer coefficient versus superficial gas velocity. Influence of the carbon chain length of alcohol.

Fig. 11 shows the increase in K_La versus the superficial gas velocity. This figure also illustrates that the K_La values decrease as the number of carbons in the alcohols increases. A pronounced decrease of K_La is observed with the anionic surfactant (SDS).

In alcohol or ionic surfactant solutions, there is an excessive concentration of alcohol or ionic surfactant in the gas-liquid interface. A dynamic rise in the surface tension in the gas-liquid interface is induced due to the bubble movement through the liquid. In that case, a tiny addition of surfactant can strongly inhibit bubble coalescence and result in significantly smaller bubble size distribution. The interfacial coefficient a then increases because of this addition.

On the other hand, the presence of surfactants or alcohol at the liquid bubble interface decreases the diffusivity of oxygen through this interface, which reduces the transfer coefficient K_L.

In the presence of surfactant, the diffusivity of oxygen (D) can be reduced compared to the diffusivity of oxygen in clean water (D_w) in such a way that D/D_w equals 0.6 [41]. Therefore, the interfacial area increases with the increase in the number of carbons in the alcohol. This increase is even greater when using anionic surfactant (SDS). Hence, the decrease in K_La is due to the decrease in K_L and that decrease in K_L is more important than the increase of interfacial coefficient.

Models were tested to estimate the liquid side mass transfer

coefficient (K_L). First, the double film theory was tested to determine K_L. The mass transfer coefficient may be estimated such as the convective mass transfer film coefficient:

$$K_L=(D_L/d_B)\,Sh \tag{20}$$

where D_L is the mass diffusivity and Sh is the Sherwood number. The Sherwood number, the ratio of the convective mass transfer to the rate of diffusive mass transfer, can be determined by using the equation [42]:

$$Sh=2+0.552\,Re^{1/2}\,Sc^{1/3} \tag{21}$$

where $Re=U_b\,d_B/\nu_l$; U_b: bubble rise velocity, d_B: bubble diameter, ν_l: kinematic viscosity; Sc: Schmidt number$=\nu_l/D_l$; D_L is the molecular diffusion of oxygen in liquid.

This model underestimates the experimental results. Thus, with this model, we obtain for water, for example: $K_La=0.0015$ 1/s for $U_g=1.83$ cm/s and $K_La=0.0057$ 1/s for $U_g=6.3$ cm/s.

The interfacial coefficient a is expressed as:

$$a=6\frac{\varepsilon_g}{d_B}. \tag{22}$$

Then Higbie's theory was tested. Depending on the nature of the bubble in terms of full mobility or rigidity of bubble, Higbie's theory of penetration can be expressed to determine the liquid-side mass transfer coefficient [43].

For a fully mobile bubble as in the case of pure water, the following expression is used:

$$K_L^{mobile}=\frac{2}{\sqrt{\pi}}\sqrt{\frac{D_L U_r}{d_B}}=1.13\sqrt{\frac{U_r}{d_B}}D_L^{1/2} \tag{23}$$

where U_r is the bubble - liquid relative velocity (slip velocity).

For the bubble with a rigid surface as in a contaminated liquid, the liquid-side mass transfer coefficient can be predicted using an equation proposed by Frössling [42] and Griffith [44] from the laminar boundary layer theory. In this case, the following expression is used:

$$K_L^{rigid}=0.6\sqrt{\frac{U_r}{d_B}}D_L^{2/3}\nu_L^{-1/6} \tag{24}$$

By approximating U_r by U_g/ε_g and taking d_B varying from 4 mm to 6 mm (average diameter: from photos) for the case of a mobile bubble and d_B varying from 2 to 2.5 mm for a rigid bubble, K_L was calculated according to Eqs. (22) and (23).

Table 4 summarizes these results showing that the values of K_L decrease as the number of carbons increases. With the values obtained for K_L, it was possible to obtain values of K_La close to the experimental values, especially with alcohols. For SDS, Higbie's model overestimates K_La. This proves that by taking into account the rigidity or the mobility of the surfaces of the bubbles, Higbie's theory can approach the experimental results.

The increase in the surface tension gradient can be taken as an indication of a strong presence of surfactant or alcohol molecules at the liquid bubble interface. Therefore, the decrease in K_L can be correlated with this surface tension gradient.

A regression analysis of the data was undertaken to develop a correlation that can be used for design and scale-up purposes. This correlation is useful in aqueous solutions of alcohols having a short carbon chain and in anionic surfactant solution. Data for gas-liquid mass transfer coefficient K_La can be correlated to gas hold-up and surface tension gradient to represent the effect of the dynamic surface tension.

The following correlation was found to represent the experimental volumetric mass transfer results in semi pilot bubble column for both systems (air-pure water, air-water-alcohol mixture and SDS solution):

$$K_La=0.0221\,\varepsilon_g^{1.17}\left|\frac{d\sigma}{dx}\right|^{-0.053} \tag{25}$$

Table 5 shows this correlation with standard deviation. The latter is not exceeding 14%.

A comparison of present values of K_La with available data and correlations provided in literature is presented in Fig. 12.

For pure water (tap water) and propanol 0.05% aqueous solutions, the values of K_La found by Gourich et al. [45] are in general slightly higher than in the present work. The internal diameter of the column used by these researchers is 10 cm, while that used in the present work is 19.4 cm. Besides, the identification of K_La was based on a perfectly mixed reactor model without any RTD study

Table 4. Predicted values of liquid-side mass transfer coefficient (Higbie's theory)

U_g (cm/s)	10^4 K_L (m/s) pure water	10^4 K_L (m/s) Ethanol 0.05%	10^4 K_L (m/s) 2-Propanol 0.05%	10^4 K_L (m/s) 1-Butanol 0.05%	10^4 K_L (m/s) SDS 0.001 M
1.83	4.45	0.804	0.79	0.67	0.65
2.94	4.3	0.811	0.71	0.594	0.57
4.3	4.26	0.827	0.709	0.596	0.58
6.3	4.58	0.876	0.767	0.65	0.6

Table 5. Correlations of K_La for 0.6%<ε_g<15% ($d\sigma/dx$ is expressed in N/m)

Correlation	Standard deviation			
$K_La=0.0221\,\varepsilon_g^{1.17}\left\|\frac{d\sigma}{dx}\right\|^{-0.053}$	Ethanol	Propan-2-ol solution 0.05%	Butan-1-ol solution 0.05%	SDS solution 10^{-3} mol/L
	13.8%	9%	11.6%	13%

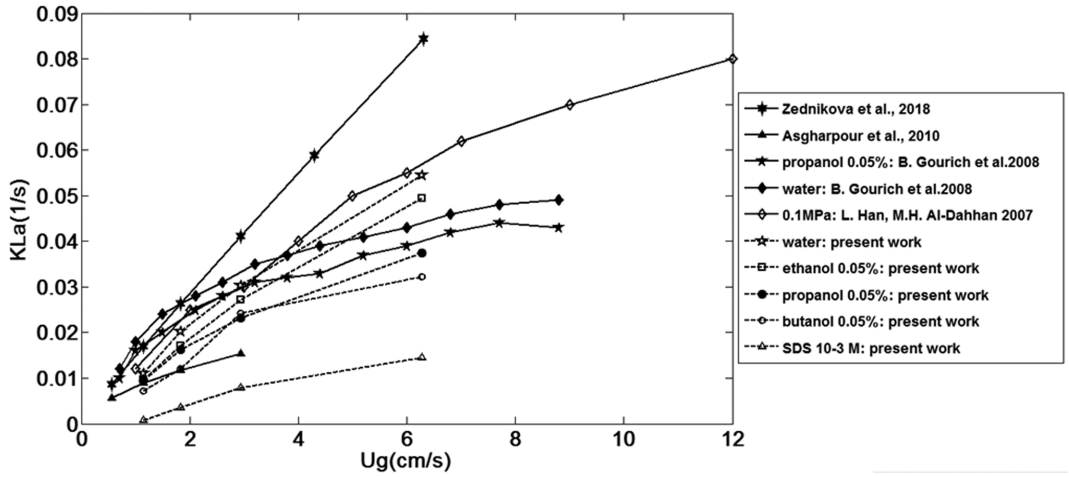

Fig. 12. Dependence of volumetric mass transfer coefficient on corresponding superficial gas velocity: Comparison of present data with available correlations provided in literature.

to prove this aspect of the flow.

Similar values were obtained for pure water solutions as found by Han and Al-Dahhan [46]. They showed that although the K_La values increased with the operating pressure, the pressure change from 0.1 to 0.4 MPa yielded lower K_L values as a result of the reduced bubble size.

The correlation proposed by Zedníková [47] overestimates the values of K_La (pure water) of the present work and of those of other authors. In their correlation, K_La is directly correlated with U_g: $K_La=1.144\ U_g^{0.943}$. The tap water used in the present work acts also as surfactants allowing to a decrease of K_L because of the surface tension gradient. So the values of K_La obtained for distilled water should be higher than those of tap water.

The effect of surfactant (SDS) on K_La in a distilled water system and 0.1% tridecane-water system as a function of gas velocity is also observed in the comparison curves [48]. The correlation proposed by these authors is: $Sh=0.15\ Re^{2/3}\ Sc^{1/2}\ Bo^{2/3}$.

Sh: Sherwood number=$K_La\ d_B^2/D_m$, D_m: diffusion coefficient (m^2/s).

The influence of surface tension is included in Bond number: $Bo=\rho_m g d_B^2/\sigma_m$.

σ_m: interfacial tension of the mixture (N/m)

ρ_m: density of the mixture (kg/m^3)

$Re=\rho_m\ U_g\ d_B/\mu_m$, μ_m: kinematic viscosity (m^2/s).

The same conclusion was found by Asgharpour et al. [48]. Thus, with the addition of surfactant to hydrocarbon in the water system, the mass transfer coefficient decreases. The presence of surfactants over a gas-liquid interface increases the interfacial area at constant gas hold-up (by reducing the average bubble diameter) but decreases the mass transfer coefficient K_L by increasing the liquid phase mass transfer resistance.

CONCLUSION

This study has shown the use of simultaneous pressure and conductivity sensors to obtain the gas hold-up in different zones as a first step, and then to determine the liquid flow pattern and RTD in case of a weak liquid flow-rate as a second step. The increase of the number of carbons in the alcohol and the presence of an anionic surfactant (SDS) leads both to an increase in the gas hold-up and to a decrease of induced liquid velocity circulation. The presence of gas is more important in the zone farther to the gas distributor (zone II).

The correlation of gas hold-up, considering the effect of surface tension gradient, represents the experimental results as the standard deviation is relatively weak in the whole range of the gas velocity used (from 0.056 to 9.7 cm/s). The determination of the overall liquid velocity was deduced through the tracer technique in the case of batch liquid phase, while in the case of continuous liquid phase, the RTD revealed that the bubble column could be modeled as a perfect mixed reactor, even at a relatively gas velocity as the Peclet number is between 1 and 4. The gas liquid mass transfer coefficient has been discussed in terms of the accuracy of the estimation of K_La. The results revealed that K_La decreases with the introduction of SDS and with the addition of alcohol, especially when the number of carbones in alcohols has increased.

In light of Higbie's theory, it has also been proven that the decrease in K_La was due to a decrease in K_L which resulted in a drop of the bubble rise velocity and the diffusivity when alcohol or ionic surfactant was added. A correlation based on the dynamic surface tension has been proposed linking the gas hold-up and the gas liquid mass transfer coefficient to superficial gas velocity and surface tension gradient.

ACKNOWLEDGEMENTS

Authors would like to acknowledge the financial support from a specific university research fund of the Ministry of Education.

DECLARATION OF INTEREST STATEMENT

The authors state that no financial relationship connects them with individuals or organizations that can influence the results of their work. The work presented is the result of a purely scientific effort.

REFERENCES

1. F. Azizi and A. M. Al Taweel, *Chem. Eng. Sci.*, **62**, 7436 (2007).
2. B. Magolan, N. Lubchenko and E. Baglietto, *Chem. Eng. Sci.: X*, **2**, 100009 (2019).
3. M. Y. Chisti, *Airlift bioreactors*, Elsevier, New York (1989).
4. E. Camarasa, C. Vial, S. Poncin, G. Wild, N. Midoux and J. Bouillard, *Chem. Eng. Process.*, **60**, 329 (1999).
5. C. Vial, E. Camarasa, S. Poncin, G. Wild, N. Midoux and J. Bouillard, *Chem. Eng. Sci.*, **55**, 2957 (2000).
6. H. Jin, S. Yang, G. He, Z. Guo and Z. Tong, *Chem. Eng. Sci.*, **60**, 5955 (2005).
7. A. Erfani, S. Khosharay and P. A. Clint, *J. Chem. Thermodyn.*, **135**, 241 (2019).
8. E. M. Cachaza, M. E. Díaz, F. J. Montes and M. A. Galán, *Chem. Eng. Sci.*, **66**, 4047 (2011).
9. G. De Guido and L. A. Pellegrini, *Chem. Eng. Res. Des.*, **124**, 283 (2017).
10. G. Besani and F. Inzoli, *Chem. Eng. Sci.*, **170**, 270 (2017).
11. C. O. Vandu and R. Krishna, *Chem. Eng. Process.*, **43**, 987 (2004).
12. A. S. Mirón, F. C. C. Camacho, A. C. Gomez, E. M. Grima and Y. Chisti, *AIChE J.*, **46**, 1872 (2000).
13. B. Gourich, C. Vial, A. H. Essadki, F. Allam, S. M. Belhaj, M. Ziyad and H. Delmas, *Chem. Eng. Process.*, **45**, 214 (2006).
14. M. Martín, F. J. Montes and M. A. Galán, *Chem. Eng. J.*, **128**, 21 (2007).
15. O. Ramazan and D. Gülbeyi, *Chem. Eng. Res. Des.*, **109**, 477 (2016).
16. P. Kováts, D. Thévenin and K. Zähringer, *Int. J. Multiphase Flow*, **123**, 103174 (2020).
17. S. Shu, D. Vidal, F. Bertrand and J. Chaouki, *Renew. Energy*, **141**, 613 (2019).
18. T. A. Dolenko, S. A. Burikov, S. A. Dolenko, A. O. Efitorov, I. V. Plastinin, V. I. Yuzhakov and S. V. Patsaeva, *J. Phys. Chem.* A, **119**, 10806 (2015).
19. K. Guo, T. Wang, G. Yang and J. Wang. *J. Chem. Technol. Biotechnol.*, **92**, 432 (2017).
20. S. R. Syeda, A. Afacan and K. T. Chuang, *Can. J. Chem. Eng.,* **80**, 44 (2002).
21. D. Rosso, D. T. Huo and M. K. Stenstrom, *Chem. Eng. Sci.*, **61**, 5500 (2006).
22. S. S. Alves, S. P. Orvalho and J. M. T. Vasconcelos, *Chem. Eng. Sci.*, **60**, 1 (2005).
23. J. Solsvik and H. A. Jakobsen, *J. Dispersion Sci. Technol.*, **35**, 1626 (2014).
24. T. O. Oolman and H. W. Blanch, *Chem. Eng. Commun.*, **43**, 237 (1986).
25. J. Zahradnik, M. Fialova and V. Linek, *Chem. Eng. Sci.*, **54**, 4757 (1999).
26. T. Fujimoto, *Sanyo Chemical Industries Ltd.*, Kyoto (Japan) (1985).
27. J. M. T. Vasconcelos, S. P. Orvalho and S. S. Alves, *Am. Inst. Chem. Engineers J.*, **48**, 1145 (2002).
28. J. Boussinesq, *Annales de Chimie et de Physique*, **29**, 364 (1913).
29. F. H. Garner and D. Hammerton, *Chem. Eng. Sci.*, **3**, 1 (1954).
30. S. S. Dukhin, V. I. Kovalchuk, G. G. Gochev, M. Lotfi, M. Krzan, K. Malysa and R. Miller, *Adv. Colloid Interface Sci.,* **222**, 260 (2015).
31. S. R. Syeda and M. J. Reza, *Chem. Eng. Res. Des.*, **89**, 2552 (2011).
32. S. Khoshray, M. Talebi, T. S. Akbari and S. T. Salehi, *J. Mol. Liq.*, **249**, 245 (2018).
33. D. R. Torn and G. M. Nathanson, *J. Phys. Chem. B*, **106**, 8064 (2002).
34. F. Biscay, A. Ghoufi and P. Malfreyt, *J. Chem. Phys.*, **134**, 044709 (2011).
35. B. Albijnic, S. Chatterjie, N. Subasinghe and M. A. W. Asad, *Chem. Eng. Res. Des.*, **113**, 241 (2016).
36. J. Zahradník and M. Fialová, *Chem. Eng. Sci.*, **51**, 2491 (1996).
37. J. Zahradník, M. Fialová, M. Růžička, J. Drahoš, F. Kăstánek and N. H. Thomas, *Chem. Eng. Sci.*, **52**, 3811 (1997).
38. O. Levenspiel, *Chemical reaction engineering*, Third Ed. John Wiley & Sons, New York (1999).
39. A. H. Essadki, B. Gourich, C. Vial and H. Delmas, *Chem. Eng. Sci.*, **66**, 3125 (2011).
40. M. K. Stenstrom and R. G. Gilbert, *Wat. Res.,* **15**(6), 643 (1981).
41. M. Jamnongwong, K. Loubière, N. Dietrich and G. Hebrard, *Chem. Eng. J.*, **165**, 758 (2010).
42. N. Frössling, *Gerlands Beitage zur Geophysik*, **52**, 170 (1938).
43. M. Rocio, S. Rui and S. S. Alves, *Chem. Eng. Sci.*, **62**, 6747 (2007).
44. R. M. Griffith, *Chem. Eng. Sci.*, **17**, 1057 (1962).
45. B. Gourich, Ch. Vial, N. El Azher, M. Belhaj Soulami and M. Ziyad, *Biochem. Eng. J.*, **39**, 1 (2008).
46. L. Han and M. H. Al-Dahhan, *Chem. Eng. Sci.*, **62**, 131 (2007).
47. M. Zedníková, S. Orvalho, M. Fialová and M. Růžička, *Chem. Eng.*, **2**, 19 (2018).
48. M. Asgharpour, M. R. Mehrnia and N. Mostoufi, *Biochem. Eng. J.*, **49**, 351 (2010).

APPENDIX

The concentration evolution of oxygen is governed by the following equation:

$$\frac{dC_L}{dt} = K_L(C_L^* - C_L) \tag{1}$$

The dynamics of the probe relative to the actual concentration (C_L) in the liquid is modeled by a first-order response which takes into account the delay:

$$\frac{dC_P}{dt} = K_p(C_L - C_p) \tag{2}$$

So:

$$L\left(\frac{dC_L}{dt}\right) = L[K_L a(C_L^* - C_L)] \tag{3}$$

$$pC_L(p) - C_p(0) = K_L a \cdot [L(C_L^*) - L(C_L(t))] \tag{4}$$

$$C_L(p) = \frac{\frac{K_L a \cdot C^*}{p} + C_L(0)}{p + K_L a} \tag{5}$$

$$L\left(\frac{dC_p}{dt}\right) = L[K_p(C_L - C_p)] \tag{6}$$

$$pC_p(p) - C_p(0) = K_p[C_L(p) - C_p(p)] \tag{7}$$

$$C_P(p)=\frac{K_P\cdot C_L(p)+C_P(0)}{p+K_P} \tag{8}$$

The expression of $C_L(p)$ (Eq. (5)) is introduced in Eq. (8):

$$C_P(p)=\frac{\dfrac{K_P\cdot K_La\cdot C^*}{p}+K_PC_L(0)}{(p+K_P)\cdot(p+K_La)}+\frac{C_p(0)}{(p+K_P)} \tag{9}$$

$$C_P(p)=\frac{K_P\cdot K_La\cdot C}{p\cdot(p+K_P)\cdot(p+K_La)}+\frac{K_PC_L(0)}{p\cdot(p+K_P)\cdot(p+K_La)}+\frac{C_p(0)}{(p+K_P)} \tag{10}$$

The inverse Laplace transform allows us to:

$$\begin{aligned}L^{-1}\left\{\frac{K_P\cdot K_La\cdot C}{p\cdot(p+K_P)\cdot(p+K_La)}\right\}&=L^{-1}\left\{\frac{1}{[p(1+T_1p)(1+T_2p)]}\right\}\\&=\left\{1-\left(\frac{1}{T_1-T_2}\right)(T_1e^{-t/T_1}-T_2e^{-t/T_2})\right\}\end{aligned} \tag{11}$$

with: $T_1=1/K_La$; $T_2=1/K_p$

and

$$\begin{aligned}L^{-1}\left\{\frac{K_PC_L(0)}{p\cdot(p+K_P)\cdot(p+K_La)}\right\}&=\frac{K_P\cdot C_L(0)}{K_La-K_P}\cdot L^{-1}\left\{\frac{1}{p+K_P}+\frac{1}{p+K_La}\right\}\\&=\frac{K_P\cdot C_L(0)}{K_La-K_P}\{e^{-K_P\cdot t}-e^{-K_La\cdot t}\}\end{aligned} \tag{12}$$

$$L^{-1}\left\{\frac{C_p(0)}{(p+K_P)}\right\}=C_p(0)\cdot e^{-K_P\cdot t}$$

We can deduce:

$$\begin{aligned}\frac{C_p(t)}{C_p^*}&=\left\{1-\left[\frac{1}{T_1-T_2}\right][T_1e^{-K_La\cdot t}-T_2e^{-K_P\cdot t}]\right\}\\&+\frac{K_pC_L(0)}{(K_La-K_p)}[e^{-K_La\cdot t}-e^{-K_P\cdot t}]+C_p(0)e^{-K_P\cdot t}\end{aligned} \tag{13}$$